# Electronic Modulation by Interfacial Bridging Between Ir Nanoparticle and Metal-Organic Framework to Enhance Hydrogen Evolution

Kaipeng Cheng[a], Yinghuan Xu[a], Shenmeng Zhang[a], Heng Zhang[c*], Yingying Xue[a], Xiahui Huang[a], Jianbo Zhao[b], Pengcheng Zhang[a], Shuang Ma[d*], Zhiqiang Hou[a*]

a School of Chemistry and Chemical Engineering, Zhoukou Normal University, Zhoukou 466000, PR China;

b School of Chemistry and Chemical Engineering, Tarim University, Alar 843300, PR China

c Science Island Branch of Graduate School, University of Science and Technology of China, Hefei, 230026, P. R. China

d School of Chemical & Environmental Engineering (Key Lab of Ecological Restoration in Hilly Areas), Pingdingshan University, Pingdingshan, 467000, P.R. China

# 1. Experimental Section

## 1.1 Materials and reagent

Cobalt (II) nitrate hexahydrate ($Co(NO_3)_2 \cdot 6H_2O$), Terephthalic acid (BDC), N,N-Dimethylformamide (DMF) and ethanol were purchased from Aladdin Industrial Corporation. $IrCl_3$ was purchased from Acmec. 5% Nafion solution, Platinum powder (Pt/C, 20wt%) and Iridium powder (Ir/C, 10wt%) was provided by Sigma Aldrich Corporation. Ni Foam with a thickness of 1.6 mm and 120 ppi (pore per square inch) was purchased from Jia Shide Foam Metal Co., Ltd (Suzhou, China). All chemical reagents were used without any further purification.

## 1.2 Preparation of Co-MOF

The Co-MOF was synthesized by a typical solvothermal procedure. Firstly, The 1 cm × 2 cm nickel foam underwent multiple rounds of washing with 3 M hydrochloric acid, acetone, and ethanol. 0.3 mmol of $Ni(NO_3)_2 \cdot 6H_2O$ and 80 mg of Terephthalic acid were first dissolved in a mixed solvent of 12 mL DMF and 1 mL deionized water. Subsequently, the obtained solution and NF was transferred into 25 mL of Teflon-lined autoclave and heated at 130 ºC for 12 h. After cooling to room temperature, Co-MOF was obtained in situ on NF, and the sample was repeatedly washed with anhydrous ethanol. Finally, the sample was dried at 60 ºC in a vacuum oven.

## 1.2 Preparation of Ir@Co-MOF

Disperse 5 mg of $IrCl_3$ in 15 mL of anhydrous ethanol and stir vigorously. The solution and Co-MOF grown on NF were then transferred to a 25 mL Teflon-lined autoclave and heated at 100 °C for 10 hours. After cooling down to room temperature,

washed with absolute ethanol, and then dried under vacuum at 60 °C overnight. To investigate the impact of the synthesis method on performance, we incorporated IrCl$_3$ during the MOF synthesis. For comparison, Co-MOF containing different Ir loads were synthesized by changing the content of IrCl$_3$ (1 and 10 mg), respectively. Two additional materials are synthesized by replacing Benzene-1,4-dicarboxylate (BDC) with Biphenyldicarboxylate (BPDC) and Benzene-1,3,5-tricarboxylate (BTC).

## 1.3 Materials characterization

The morphology and structure of the synthesized MOFs are characterized by field emission scanning electron microscopy (FESEM, JSM-6700F), transmission electron microscopy (TEM, JOEL, JEM-2010, Talos F200X), powder X-ray diffractor (XRD, TTR-III), micropore and chemisorption analyzer (Micrometritics, ASAP 2020). The chemical state of the sample was performed on X-ray photoelectron spectroscopy (XPS, ESCALAB 250, UK), the Fourier transform infrared spectroscopy (FT-IR, Nicolet 8700, USA) and confocal Raman microscope (LabRam HR, Horiba Yobin Yvon) with a 30 mW He/Ne laser (633 nm) as the excitation source. The XAFS spectra at the Ru K-edge were recorded at the BL11B beamline of Shanghai Synchrotron Radiation Facility (SSRF). The incident photons were monochromatized by a Si(311) double-crystal monochromator. The energy calibration was performed using a Co reference foil.

## 1.4 Electrochemical measurements

Electrochemical measurements were performed with a workstation (CHI 660E, Shanghai, China) in a typical three-electrode configuration consisting of a platinum wire (the counter electrode), Hg/HgO (the reference electrode) and the active material

(the working electrode) in 1.0 M KOH solution. The loads of Co-MOF and Ir@Co-MOF are 1.24 and 1.16 mg cm$^{-2}$, respectively. The measured potentials were given according to the following formula: E(RHE) = E(Hg/HgO) + 0.059 × pH + 0.098. Linear sweep voltammetry (LSV) and cyclic voltammetry (CV) measurements were performed to evaluate the HER properties of catalysis. For comparison, a benchmark Pt/C and Ir/C catalyst on Ni foam was fabricated by the following steps: 784 μL ethanol, 20 μL Nafion, 196 μL deionized water and 5 mg Pt/C were mixed to prepare dispersion and sonicated for 30 minutes. Finally, a certain of prepared dispersion was add on the NF.

The linear sweep voltammetry (LSV) curves were recorded with a scan rate of 5 mV s$^{-1}$. The Tafel slope was calculated by fitting the linear portion of the Tafel plots, obtained by using the Tafel equation [$\eta$ = b log(j) + a]. And all the polarization curves were corrected by the iR-drop compensation. The electrochemical impedance spectroscopy (EIS) was performed to cover the frequency interval from 0.01 Hz to 100 kHz with a 10 mV amplitude.

Electrochemical capacitance measurements were used to determine the active surface area of each catalyst. To estimate the electrochemical active surface area of the electrocatalysts, double-layer capacitance ($C_{dl}$) was considered in the non-faradaic region (-0.8 ~ -0.9 V vs. Hg/HgO) of CVs recorded at different scan rates of 10, 20, 30, 40 and 50 mV s$^{-1}$. Finally, the ECSA was obtained through dividing $C_{dl}$ by the specific capacitance of electrode material. Generally, the specific capacitance for flat surface electrodes is 0.06 mF cm$^{-2}$.

### 1.3.1 Turnover frequency (TOF) calculations

The TOF ($s^{-1}$) values were calculated with the following equation: TOF = I/mnF

I: Current (A) during the linear sweep voltammetry (LSV) tests in 1 M KOH.

n: Number of active sites (mol). F: Faraday constant ($C\ mol^{-1}$).

m: The factor 1/m represents that m electrons are required to form one $H_2/O_2$ molecule from water, which means that the m values for oxygen evolution reactions are 4.

Number of Active sites calculations (n):

According to the formula described in the experimental section:

$$n = Q/2F = It/2F = IV/2Fv$$

where Q is the voltammetric charge, F is the Faraday constant ($C\ mol^{-1}$), I stands for the current (A), t is the time (s), V is the voltage (V) and v is the scanning rate ($V\ s^{-1}$).

### 1.3.2 Faradaic efficiency

The Faradaic efficiency (FE) of HER catalysts is defined as the ratio of the amount of experimentally determined $H_2$ (ne) to that of the theoretically expected $H_2$ (nt) from the reaction:

$$FE = \frac{n_e}{n_t}$$

Theoretical amount of $H_2$ was calculated by applying Faraday Law:

$$n_t = \frac{JAt}{2F}$$

## 2. DFT Computational method

Density functional theory (DFT) calculations were performed using a Dmol3 program package of software Materials Studio 2020. The Perdew-Burke-Ernzerhof (PBE) function of the generalized gradient approximation (GGA) was used to account

for electron exchange and correlation.[1] The computational parameters were self-consistent field (SCF) tolerance $1.0 \times 10^{-7}$ Ha per atom, energy tolerance $2.0 \times 10^{-7}$ Ha per atom, maximum force gradient 0.002 Ha $\text{Å}^{-1}$, maximum atomic displacement 0.005 Å, orbital cutoff 4.6 Å and thermal smearing 0.01 Ha for quick convergence.

The Gibbs free energies of hydrogen adsorption ($\Delta GH^*$) were calculated as follow:

$$\Delta G_{H^*} = \Delta E_{H^*} + \Delta E_{ZPE} - T\Delta S$$

Where $\Delta E_{H^*} = E(\text{slab}+H^*) - E(\text{slab}) - E_{H2}/2$, $\Delta E_{ZPE}$ stands for the change in zero-point energy and $\Delta S$ represents the entropy change.[2] Norskov et al. previously reported that $\Delta E_{ZPE} - T\Delta S$ is approximately 0.24 eV.[3] Therefore, we take $\Delta G_{H^*} = \Delta E_{H^*} + 0.24$ eV.

1. J.P. Perdew, K. Burke, M. Ernzerhof, Generalized gradient approximation made simple, *Phys Rev. Lett.,* 1996,**77**, 3865.

2. L. Ou, F. Yang, Y. Liu, S. Chen, First-Principle Study of the Adsorption and Dissociation of $O_2$ on Pt(111) in Acidic Media, *J Phys Chem C,* 2009, **13**, 20657-20665.

3. Nørskov JK, Bligaard T, Logadottir A, Kitchin J, Chen JG, Pandelov S, Stimming U, Trends in the exchange current for hydrogen evolution, *J Electrochem Soc,* 2005, **152**, J23.

# Figure
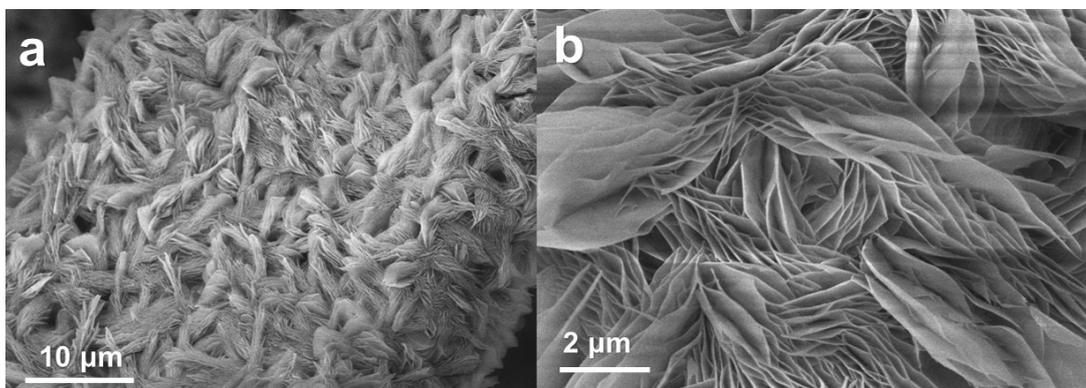


Fig. S1. SEM image of Co-MOF.
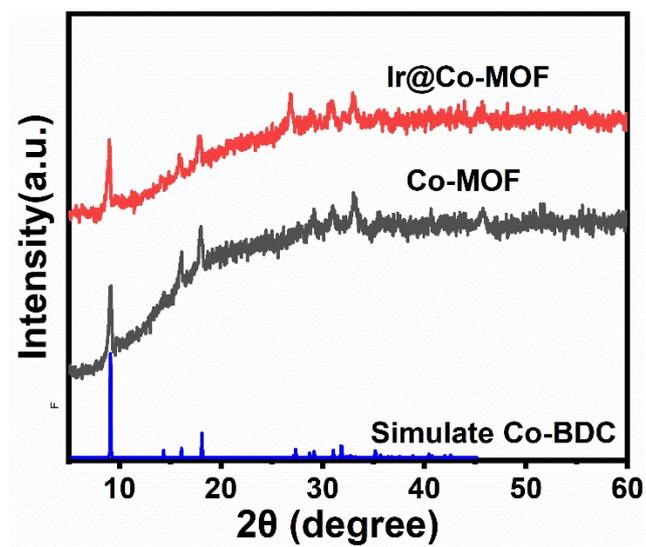


Fig. S2. XRD pattern of Ir@Co-MOF and Co-MOF.
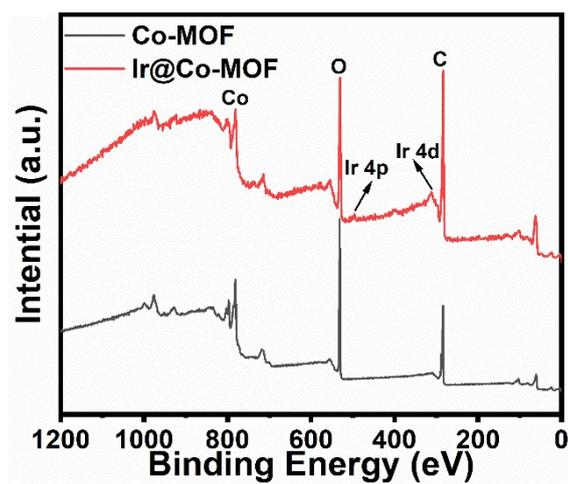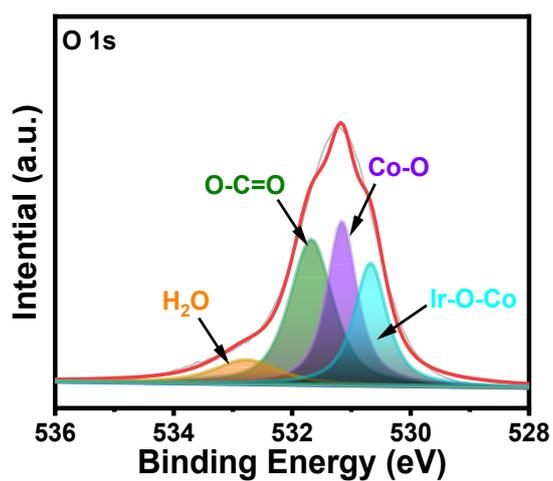
Fig. S3. XPS spectra of Ir@Co-MOF and Co-MOF.



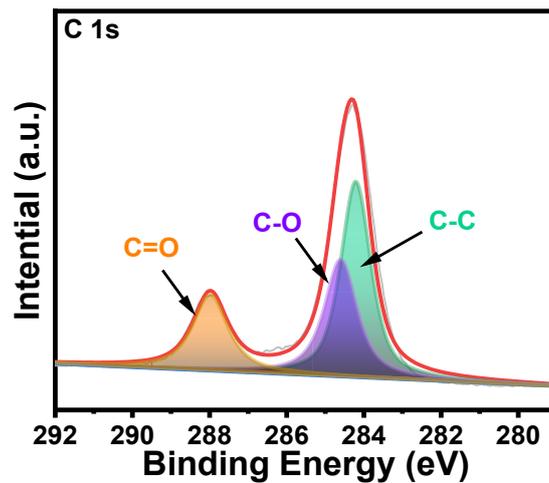Fig. S4. High-resolution O 1s spectra of Ir@Co-MOF.

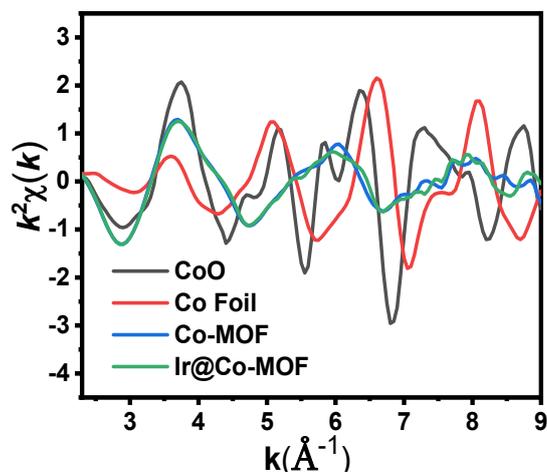Fig. S5. High-resolution C 1s spectra of Ir@Co-MOF.



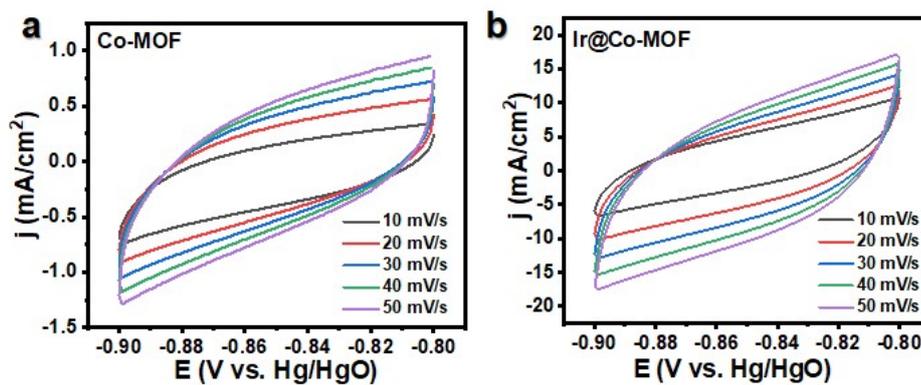Fig. S6. Co K-edge EXAFS oscillation function of Co foil, CoO, Co-MOF, and Ir@Co-MOF, respectively.

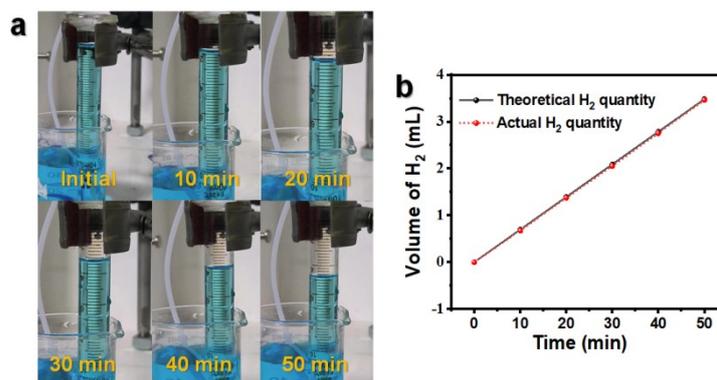Fig. S7. CV curve of electrodes recorded at different scan rates of 10, 20, 30, 50 and 50 mVs$^{-1}$ in 1 M KOH solution, for a) Co-MOF and b) Ir@Co-MOF.



Fig. S8. (a) Enlarged digital images of the measuring cylinders displayed and levels of hydrogen gas generated at 0, 10, 20, 30, 40, 50 min in 1M KOH. (b) Plot illustrating the faradaic efficiency in 1M KOH.
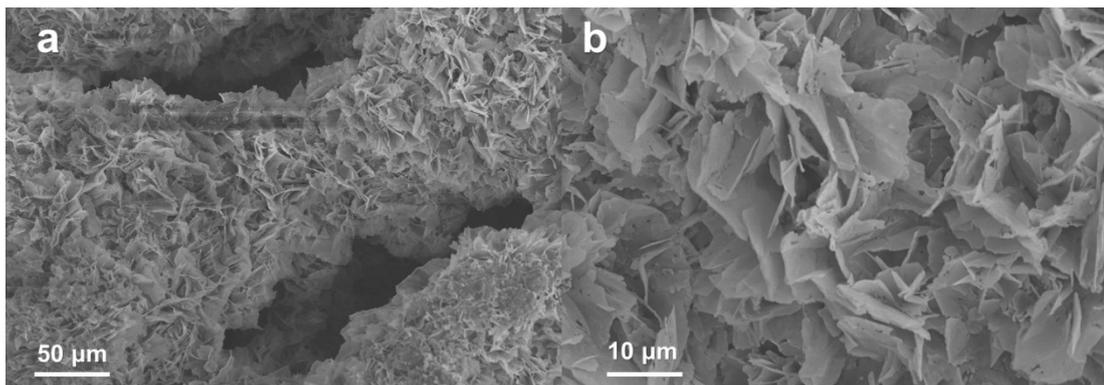
Fig. S9. SEM images of Ir@Co-MOF after HER test.
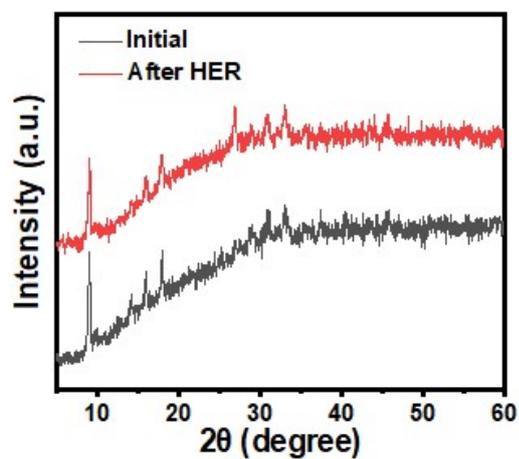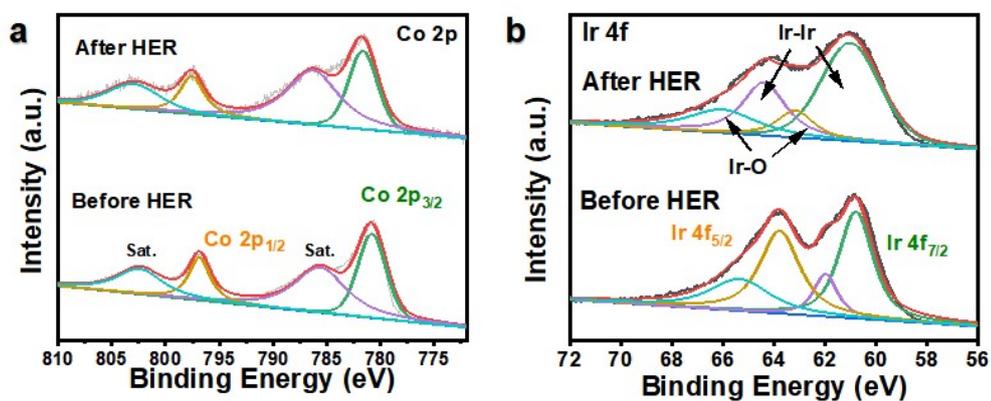


Fig. S10. XRD patterns of Ir@Co-MOF after water electrolysis test.



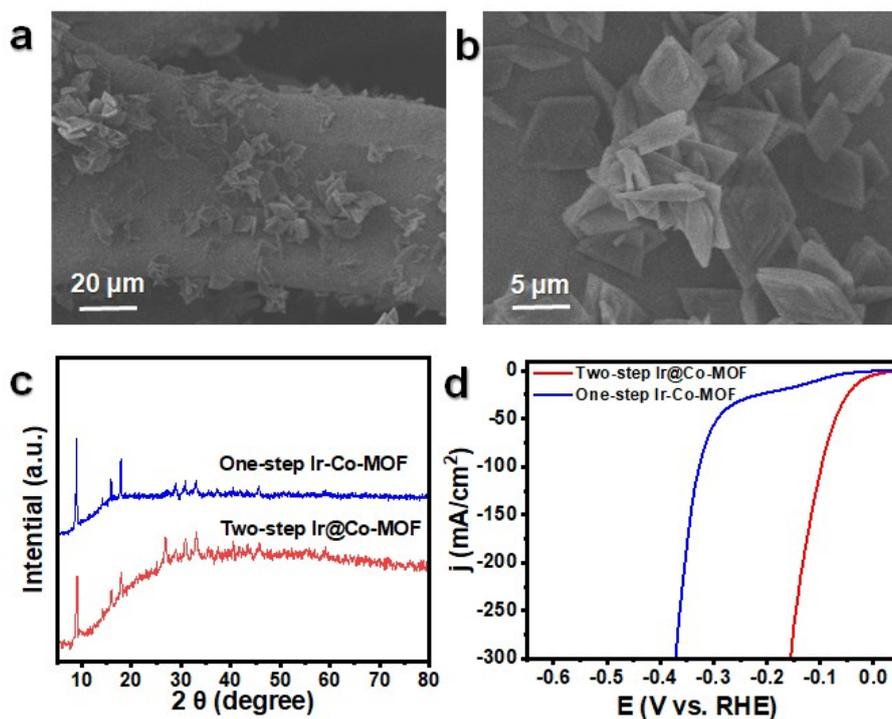Fig. S11. High-resolution (a) Co 2p and (b) Ir 4f spectra of Ir@Co-MOF after HER test.

Fig. S12. (a, b) SEM images at different magnification of Ir@Co-MOF are synthesized by one-step method; (c) Corresponding XRD pattern; (d) LSV curves of One-step Ir@Co-MOF and Two-step Ir@Co-MOF.
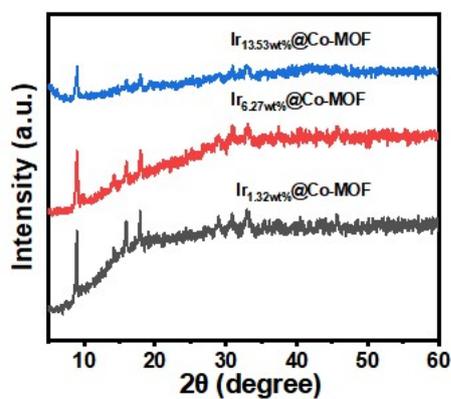


Fig. S13. XRD patterns of Ir@Co-BPDC with different Ir content.
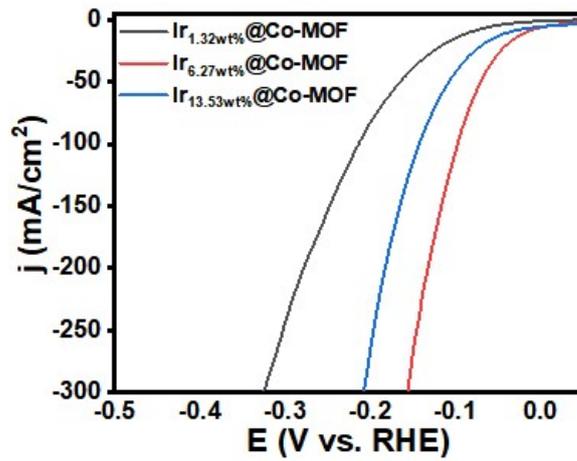
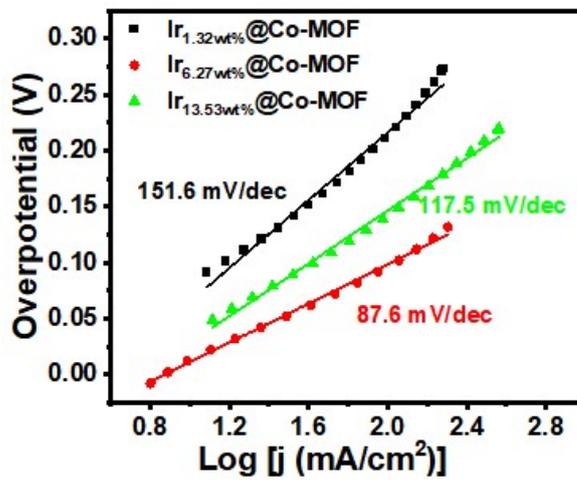Fig. S14. HER polarization curves of Ir@Co-BPDC with different Ir content.



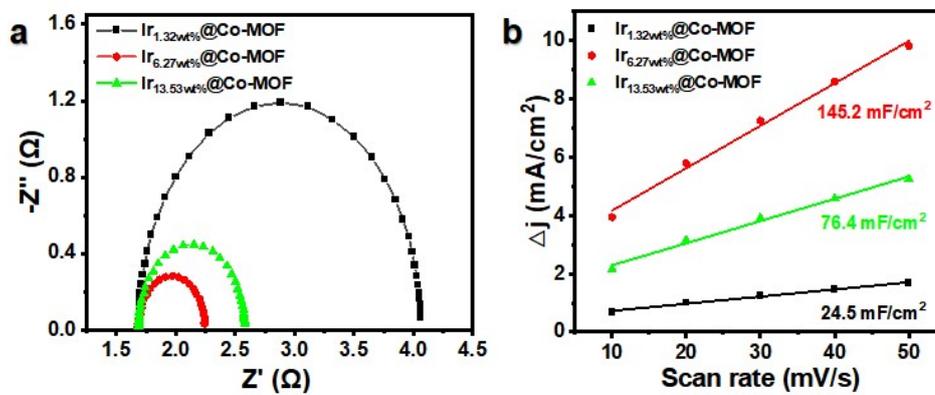Fig. S15.Tafei plots of Ir@Co-BPDC with different Ir content.



Fig. S16. Nyquist plots and the double layer capacity Cdlof Ir@Co-BPDC with different Ir content.
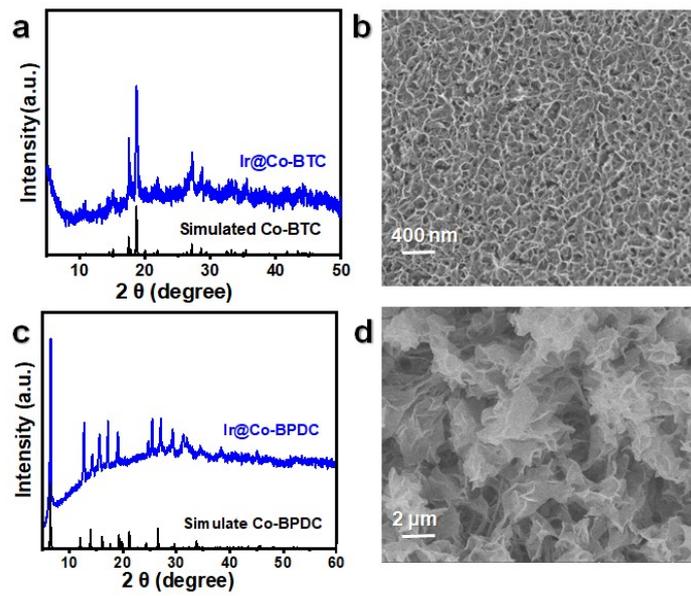
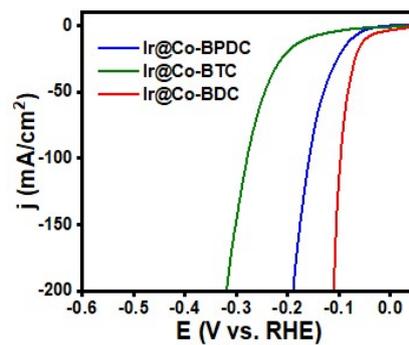Fig. S17 (a) Ir@Co-BTC XRD and (b) SEM images; (c) Ir@Co-BPDC XRD and (d) SEM images.



Fig. S18. The LSV curve of Ir@Co-BTC, Ir@Co-BPDC and Ir@Co-BDC.

**Table S1.** Comparison of the HER activity for Ir@Co-MOF with several recently reported electrocatalysts

| Catalyst | $\eta_{10}$ [mV] | Tafel slope [mV/dec] | Reference |
|---|---|---|---|
| Ir@Co-MOF | 28 | 87.6 | This work |
| Co@Ir/NC-10% | 29.4 | 41.9 | *ACS. Sustainable Chem. Eng.* **2018,** *6,* 5105-5114. |
| CoIr@CN | 70 | 123.8 | *J. Mater. Chem. A. 10 (2022) 15543－15553.* |
| IrNi-N-C | 45 | 38 | *Nano Energy 98 (2022) 107296.* |
| $IrO_2/V_2O_5$ | 75 | 48 | *Adv. Sci.* **2022,** *9,* 2104636. |
| IrCo@NC | 82 | 56 | *Adv. Funct. Mater.* **2021,** *31,* 2101797. |
| $IrP_2$@NC | 28 | 50 | *Energy Environ. Sci. 12 (2019) 952－957..* |
| $IrO_2$@$MnO_2$/rGO | 170 | 87 | ACS Sustainable Chem. Eng. 10 (2022) 15068－15081. |
| Ir 18wt% -NiO | 215 | 35 | ACS Catalysis, 2020, 10(21): 12575-12581. |
| Ir@NG-750 | 114 | 113 | *J. Mater. Chem. A.* **2020,** *8,* 19665-19673. |
| AC-SrIrO$_3$ | 139 | 49 | *Chem. Mater.* **2020,** *32,* 4509-4517. |
| Ir/N-rGO | 76 | 52.6 | Green Energ. Environ., 2022, 7(5): 1111-1118. |